AIP CONFERENCE PROCEEDINGS 205

THE PHYSICS OF ELECTRONIC AND ATOMIC COLLISIONS

XVI INTERNATIONAL CONFERENCE

NEW YORK, NY 1989

EDITORS:

A. DALGARNO
HARVARD-SMITHSONIAN CENTER FOR ASTROPHYSICS

R. S. FREUND
AT&T BELL LABORATORIES

P. M. KOCH
STATE UNIVERSITY OF NEW YORK at STONY BROOK

M. S. LUBELL
CITY UNIVERSITY OF NEW YORK, CITY COLLEGE

T. B. LUCATORTO
NATIONAL INSTITUTE OF STANDARDS AND TECHNOLOGY

AIP

American Institute of Physics **New York**

CONTENTS

PHOTONS

IONS AND ATOMS

MOLECULES

GENERAL

SYMPOSIUM: CORRELATED TRANSFER/EXCITATION AND AUTOIONIZATION

SYMPOSIUM: COLLISIONS WITH COLD PARTICLES

SYMPOSIUM: COLLISIONS INVOLVING POSITRONS

SYMPOSIUM: SUPERCOMPUTATIONAL COLLISION PHYSICS

SPECTRAL DISTRIBUTION OF ELECTRONS EMITTED INTO THE CONTINUUM OF FAST PROJECTILES: THEORETICAL APPROACHES OF HIGHER ORDER IN COMPARISON WITH EXPERIMENT

D.H.Jakubaßa-Amundsen

Physics Section, University of Munich, 8046 Garching, Germany

A compilation of recent experimental data on the forward peak resulting from the capture of target electrons into the continuum of bare, partly stripped and neutral projectiles is presented. The impact-parameter dependence and the dependence of the peak shape on the projectile charge state as well as on the angular acceptance is considered. An interpretation is attempted within the second-order Born theory and the impulse approximation. Results from Monte Carlo calculations at lower impact energies are also included.

1. Introduction

Since its discovery, the forward peak (cusp) in the secondary electron spectrum has attracted great interest both experimentally and theoretically.[1] It consists of target or projectile electrons which are emitted into low-lying continuum states of the projectile, and hence appears in the laboratory frame at forward electron angles $\vartheta_f \approx 0$ and comprises electron momenta k_f in the vicinity of the collision velocity v. Recent coincidence experiments[2] have offered the possibility to separate the contributions from target electrons (CTC) and from projectile electrons (ELC). Although a very recent compilation of ELC data[3] calls for an improvement of the theoretical approaches beyond the customary first-order Born theory, I shall restrict myself to the CTC process since it is much more sensitive to higher-order effects than the electron loss process. Starting with the derivation of the second Born theory and the impulse approximation (IA) for structured projectiles (section 2), I shall consider CTC by bare projectiles and show how the dependence of the peak shape on the angular acceptance is related to the nonanalytic behaviour of the doubly differential CTC cross section at $\vec{k}_f = \vec{v}$ (section 3). It is further shown how the variation of the peak shape with projectile charge Z_P depends on the collision velocity. The influence of the collision dynamics on the peak formation is displayed with the help of a classical trajectory Monte Carlo (CTMC) calculation[4], and the impact-parameter dependence of the forward electrons is studied within the impulse approximation. In section 4, I consider electron capture by partly stripped projectiles and show that a description of the projectile in terms of a pointlike ionic charge is incorrect. The last section is devoted to CTC by neutral projectiles where the observation of a cusp-like peak[2] is a great challenge to theory.

2. Theory

For a theoretical description of charge transfer within a perturbative approach, one has to restrict oneself to energetic collisions where the velocity v exceeds the shell velocity of the electron in its initial target bound state, or where the ratio between target charge Z_T and projectile charge Z_P deviates largely from unity. In the following I shall treat the target as a quasi one-electron system, but will take the projectile electrons (as far as they exist) explicitly into account. The neglect of multiple target excitations is especially justified for the case $Z_P/Z_T \ll 1$.

In the semiclassical picture where the internuclear motion is described by a classical trajectory, the capture amplitude is given by (in atomic units $\hbar = e = m = 1$)

$$a_{fi} = -i \int dt \langle \psi_f^{(-)} | V_i | \varphi_i^T \phi_i^P \rangle \qquad (2.1)$$

where φ_i^T is the wavefunction of the bound target electron and ϕ_i^P describes the electronic ground state of the projectile. The initial perturbation V_i is composed of the interaction V_{PT}^e of the projectile electrons with the target electron, the interaction V_{PT}^N of the projectile electrons with the target nucleus, and the interaction V_P between the projectile nucleus and the target electron. In the (prior) impulse approximation, valid for $Z_P \ll Z_T$, the exact scattering function $\psi_f^{(-)}$ is approximated by

$$|\psi_f^{(-)}\rangle = (1 + G^{(-)} V_f)|f\rangle \approx (1 + G_{IA}^{(-)} V_f)|f\rangle$$
$$|f\rangle = \sum_\lambda b_{f\lambda} |\psi_\lambda^{P+1}\rangle = \sum_{\lambda m} b_{f\lambda} |\tilde{\varphi}_{\lambda m}^P \phi_m^P\rangle \qquad (2.2)$$

where $V_f = V_T$, the potential between the target electron and the target nucleus, and consequently $|f\rangle$ eigenstate to $H_f = H - V_T$ where H is the full electronic Hamiltonian ($H = H_P + T_e + V_P + V_T + V_{PT}^e + V_{PT}^N$; H_P describes the projectile electrons, T_e the one-electron kinetic energy). The state $|f\rangle$ can be represented in terms of eigenstates ψ_λ^{P+1} to the projectile plus one electron (in absence of the target nucleus) which again can be written as a superposition of electronic states ϕ_m^P of the projectile alone, where $\tilde{\varphi}_{\lambda m}^P$ is a one-electron scattering state. The full Greens function $G^{(-)} = (i\partial_t - H - i\varepsilon)^{-1}$ of the exact formulation is in the IA replaced by $G_{IA}^{(-)}$ corresponding to $H_{IA} = H_P + T_e + V_T + V_{PT}^N$. The second-order Born approximation would result if in $G^{(-)}$, H were replaced by $H_P + T_e$.

Introducing a complete set of eigenstates $|\Phi_n^{PT}\, \vec{q}\rangle$ where $|\vec{q}\rangle$ is a one-electron plane wave of momentum $\vec{q}$ and Φ_n^{PT} eigenstate to $H_{PT} = H_P + V_{PT}^N$, and going on-shell, one obtains

$$a_{fi}^{IA} = -i \int dt \int d\vec{q} \sum_n \langle f | \Phi_n^{PT} \vec{q}\rangle \langle \Phi_n^{PT} \varphi_{\vec{q}}^T | V_i | \varphi_i^T \phi_i^P \rangle \qquad (2.3)$$

where $\varphi_{\vec{q}}^T$ is an electronic continuum target state. Expanding $\Phi_n^{PT} = \sum_\mu a_{n\mu} \phi_\mu^P$ and making use of the orthogonality properties of the eigenstates, one arrives at

$$a_{fi}^{IA} = -i \int dt \int d\vec{q} \sum_{n\lambda} b_{f\lambda}^* \sum_m \langle \tilde{\varphi}_{\lambda m}^P | \vec{q}\rangle \; a_{nm} \qquad (2.4)$$
$$* \left[a_{ni}^* \langle \varphi_{\vec{q}}^T | V_P | \varphi_i^T \rangle + \sum_\mu a_{n\mu}^* \langle \phi_\mu^P \varphi_{\vec{q}}^T | V_{PT}^e | \varphi_i^T \phi_i^P \rangle \right]$$

The expansion coefficients a_{nk} and $b_{f\lambda}$ describe projectile excitations due to the interaction V_{PT}^N with the target nucleus:

$$a_{nk} = \langle \phi_k^P | (1 + G_{PT} V_{PT}^N) | \phi_n^P \rangle$$
$$b_{f\lambda} = \langle \psi_\lambda^{P+1} | (1 + G_f V_{PT}^N) | \psi_f^{P+1} \rangle \qquad (2.5)$$

where G_{PT} corresponds to H_{PT} and G_f corresponds to H_f.

If excitation of the projectile is neglected ($a_{nk} = b_{nk} = \delta_{nk}$) the conventional form is obtained

$$a_{fi}^{IA} \approx -i \int dt \int d\vec{q} \; \langle \tilde{\varphi}_{fi}^P | \vec{q}\rangle$$
$$* \langle \varphi_{\vec{q}}^T | (V_P + \langle \phi_i^P | V_{PT}^e | \phi_i^P \rangle) | \varphi_i^T \rangle \qquad (2.6)$$

where $\tilde{\varphi}_{fi}^P$ is a one-electron scattering state to the projectile which is in the ground state ϕ_i^P.

In complete analogy, the second Born approximation reads

$$a_{fi}^{B2} \approx -i \int dt \langle \tilde{\varphi}_{fi}^P | (1 + V_T \int d\vec{q} | \vec{q}\rangle \frac{1}{i\partial_t - \frac{q^2}{2} + i\varepsilon} \langle \vec{q}|)$$
$$* (V_P + \langle \phi_i^P | V_{PT}^e | \phi_i^P \rangle) | \varphi_i^T \rangle \qquad (2.7)$$

In accordance with the omission of the internuclear potential in the transition matrix element, also the ground-state expectation value of V_{PT}^N (which only depends on the internuclear coordinate) has been omitted in (2.7).

The impulse approximation in its post form, suitable for $Z_P/Z_T \gg 1$, can be derived[5] in a similar way as (2.6) and contains an intermediate projectile eigenstate instead of the target state $\varphi^T_{\vec{q}}$.

3. CTC by bare projectiles

For bare projectiles, V^e_{PT} in (2.6) and (2.7) is zero and $\tilde{\varphi}^P_{fi}$ reduces to a Coulomb wave φ^P_f to the charge Z_P. In order to investigate the properties of the forward electrons it is instructive to look at the Fourier transform of φ^P_f at $\vec{\varkappa}_f = 0$ ($\vec{\varkappa}_f = \vec{k}_f - \vec{v}$ is the electron momentum in the projectile reference frame) which appears explicitly in the transition amplitude (2.6)

$$\varphi^{*\,P}_{\vec{\varkappa}_f}(\vec{s}) \longrightarrow \frac{Z_P}{\pi^2}\, e^{\pi\eta_f/2}\, \Gamma(1 - i\eta_f)\, \frac{1}{s^4}$$

$$\cdot \exp(-2iZ_P[\cos\vartheta_s \cos\theta'_f + \sin\vartheta_s \sin\theta'_f \cos\varphi_s]/s), \qquad \vec{\varkappa}_f \to 0 \qquad (3.1)$$

where θ'_f is the electron emission angle in the projectile frame, and $\eta_f = Z_P/\varkappa_f$.

Upon insertion into (2.6) it follows that the doubly differential cross section diverges like $\varkappa_f^{-1}$ due to the normalisation factor of the Coulomb wave. Furthermore, the dependence on θ'_f is nonanalytical because the integration variable $\vec{s} = \vec{q} - \vec{v}$ can attain the value zero[6]. Since the phase in (3.1) switches sign if one considers forward electrons with momentum below the peak ($k_f \lesssim v$, $\theta'_f = 180^\circ$) and above the peak ($k_f \gtrsim v$, $\theta'_f = 0^\circ$), the intensity of the emitted electrons is different on the two sides of the peak, leading to an asymmetric peak shape. This behaviour is, however, only visible in higher-order theories, because in the first-order OBK theory the phase information from (3.1) drops out when calculating $|a_{fi}|^2$. The asymmetry of the forward peak is clearly seen in the experiments as shown in Fig.1 in the case of O^{8+} + Ne collisions.[7]

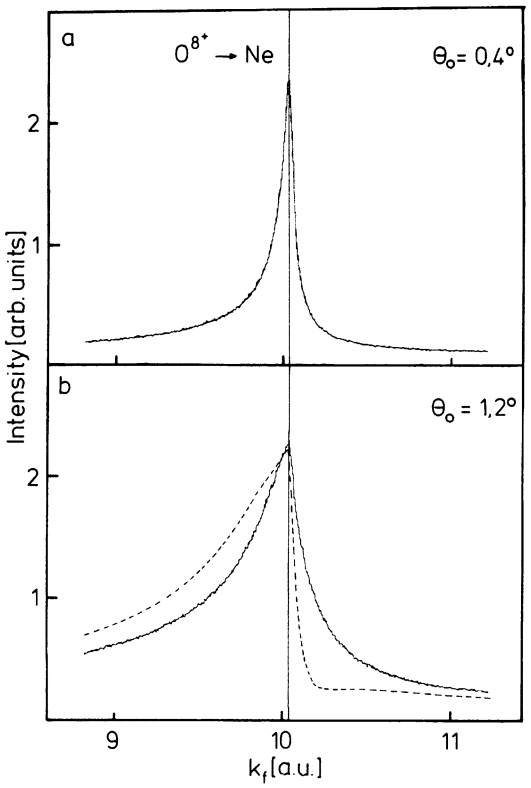

Fig.1. Cusp electron spectrum[7] from 40 MeV O^{8+} + Ne collisions at an energy resolution of 0.5% and Θ_o = 0.4° (a) and 1.2° (b). In (a), the fit by a 6-term expansion (eq. (3.2)) is indistinguishable from the data. (b) - - - - constructed "fit" with use of the same B_{1m} as for 0.4°

In order to compare theory with experiment, the differential cross section has to be averaged over the energy resolution ΔE_o and the angular resolution Θ_o of the detector. Conventionally, an expansion in terms of Legendre polynomials P_l and powers of $\varkappa_f$ is made[8]

$$\left\langle \frac{d^2\sigma}{dE_f d\Omega_f} \right\rangle_{\Theta_o, \Delta E_o} = \sum_{nl} B_{nl}\, \frac{1}{\Delta E_o} \int_{E_f - \Delta E_o/2}^{E_f + \Delta E_o/2} k_f\, dE_f$$

$$\frac{1}{1 - \cos\Theta_o} \int_0^{\Theta_o} \sin\vartheta_f\, d\vartheta_f\, \varkappa_f^{n-1}\, P_l(\cos\theta'_f) \qquad (3.2)$$

in order to extract coefficients B_{nl} which are independent of the detector resolution. However, since the cross section is nonanalytic in θ'_f a truncation of the sum over l in (3.2) is in general not possible. From Table 1 it is seen that

Θ_f'	N_1	N_2	N_3
0°	1	1	1
30°	1.02	1.01	1.05
60°	1.06	1.03	1.11
90°	1.15	1.09	1.28
120°	1.29	1.18	1.53
150°	1.42	1.27	1.79
180°	1.47	1.30	1.89

Table 1.
Cross section (in the projectile frame) for cusp electron emission at $\chi_f = 0$ within the transverse peaked prior IA. For p + He collisions with v = 4.4745, $d^2\sigma/d\varepsilon_f d\Omega_f' = N_1 * 2.02 \cdot 10^5$ barn/keV·sr, with v = 6.328, $d^2\sigma/d\varepsilon_f d\Omega_f' = N_2 * 6.43 \cdot 10^3$ barn/keV·sr, for He^{2+} + He collisions with v = 6.328, $d^2\sigma/d\varepsilon_f d\Omega_f' = N_3 * 4.57 \cdot 10^4$ barn/keV·sr

the differential cross section in the projectile frame (which results upon multiplication by χ_f/k_f) increases weakly with Θ_f' near 0° and 180°, but rather strongly around 90°. A similar result as in the IA is also found with the second Born theory. The slope is the larger, the smaller the velocity v and the larger the projectile charge. Tentative considerations indicate that the nonanalyticity reveals itself in a singular behaviour of the higher derivatives, especially around 90°.

The failure of the conventional truncation of the series to 6 terms ($l \leq 2$, $n \leq 1$) is readily seen if Θ_o is varied in the experiment. In Fig.1a where $\Theta_o = 0.4°$, the B_{1m} are fitted to the experimental spectrum. If these B_{1m} are used to construct the spectrum for e.g. $\Theta_o = 1.2°$ (Fig. 1b) a clear discrepancy with the experimental data is found.

As a measure of the peak asymmetry, the half width at half maximum to the left (Γ_L) and to the right (Γ_R) of the line $k_f = v$ can be used. In Fig.2 the ratio Γ_L/Γ_R following from experiment and from the second Born theory is shown. The experimental decrease of the peak asymmetry for $\Theta_o \to 0$ (which is another argument against a truncated series expansion) is qualitatively reproduced by theory. Note that although eq. (2.7) has

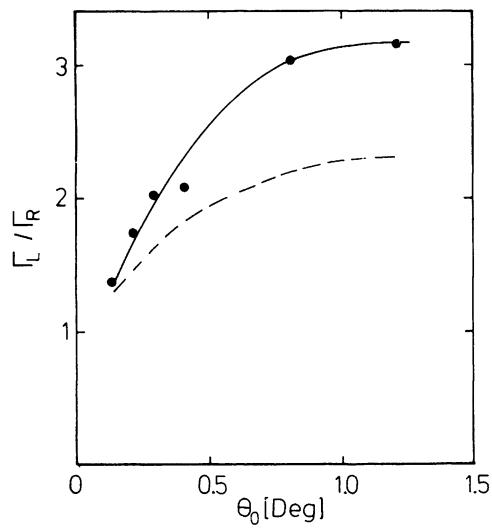

Fig.2. Ratio Γ_L/Γ_R for 40 MeV O^{8+} + Ne as a function of detector resolution[7]. Solid line, eye-guide to the data, dashed line, 2.Born

been evaluated without resorting to the asymptotic approximation of Shakeshaft[9], the second Born theory is not expected to give quantitative agreement with the data for systems with $Z_P \approx Z_T \approx v$.

The shape of the forward peak depends strongly on the system parameters like projectile charge and collision velocity. Fig.3 displays the cross section ratio for He^{2+} impact to proton impact on He at a rather low collision velocity of 2 au, and also the cross section ratio for O^{8+} impact to hydrogen impact on Ne at v = 10 au. The low-velocity data, which are well reproduced by a Monte Carlo calculation[10], scale approximately with Z_P^2 at small momenta of the ejected electron, but show an increase when $k_f > v$. This increase reflects a <u>decreasing</u> peak asymmetry with Z_P. On the other hand, the high-velocity data scale approximately with $Z_P^{2.3}$ but decrease when k_f increases beyond v. This behaviour is qualitatively explained by the (post) impulse approximation[11] (for a He target in order to obey the IA validity criterions) which scales like Z_P^3 and which leads to an asymmetry which <u>increases</u> according to Z_P/v. A similar difference in the v dependence of the asymmetry (an increase with v at small v but a

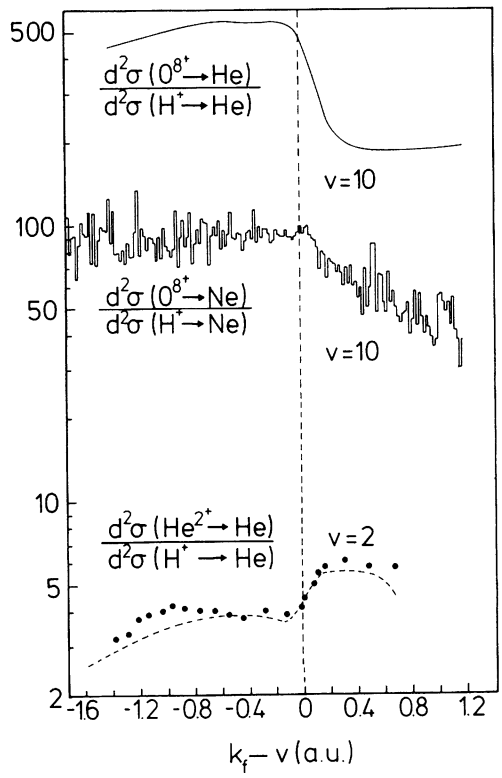

Fig.3.
(Top) Ratio of the doubly differential cross section for 2.5 MeV/N O^{8+} + Ne to H^+ + Ne collisions (exp: histogramm; $\Theta_o \sim 0.8°$, $\Delta E_o/E_f = 0.5\%$) as a function of electron momentum relative to v; solid line, cross section ratio for 2.5 MeV/N O^{8+} + He to H^+ + He at $\vartheta_f = 1°$ within the post IA. (Bottom) Cross section ratio for 100 keV/N He^{2+} + He to H^+ + He. Data points, Bernardi et al, dashed line, CTMC calculation at $\vartheta_f = 5°$ (taken from Ref. 10)

decrease at large v) has been observed by Dahl[12].

A supplementary information about the cusp electrons can be extracted from an investigation of the collision dynamics. Especially suited is the Monte Carlo method, where the classical trajectories of the projectile can be followed. In Fig.4 is shown how the forward peak develops as the internuclear distance between the proton and the He target is increased after the encounter. Distances of the order of 10^5 au are necessary in order to give the correct energy spectrum which compares well with the experimental data of Gibson[13] and Dahl[12], pointing to strong post-collisional effects in medium-energy collisions. In

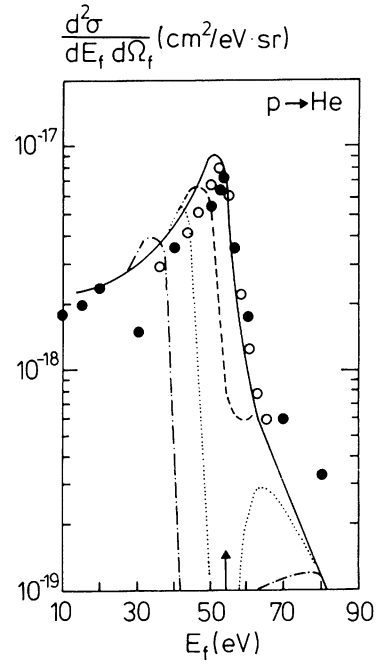

Fig.4.
Forward peak and its formation as a function of the internuclear distance R_o (where the CTMC calculation is stopped) for 100 keV p + He collisions at $\vartheta_f = 1°$. -·-·-·- , R_o = 100 au, ·····, R_o = 500 au, - - - - , R_o = 3000 au, ———, R_o = 10^5 au, Experiments: ●, Gibson and Reid[13], ○, Dahl[12] (taken from Ref.4)

quantum mechanical calculations, the information on the relevant projectile-target distances is contained in the impact parameter distribution. Fig.5 gives a comparison of the experimental data of Jagutzki et al[14] with the (prior) peaked impulse approximation[6] (which is scaled by the ratio between the unpeaked IA and the peaked IA for 1s-1s capture in the same collision at b = 0). For H^+ + Ne, theory reproduces experiment within the experimental uncertainty of the normalisation ($\sim$ 50%). A measurement of the b-distribution of δ-electrons emitted under zero degrees gives within the error bars the same shape as the b-distribution of the cusp electrons. This confirms the validity of the peaked IA which factorises into the ionisation probability times the squared normalisation constant of the final-state Coulomb wave.[6,15] For the more symmetric $^3He^{2+}$ + Ne collision, the IA gives poor results at an impact velocity as low as the electronic velocity of the

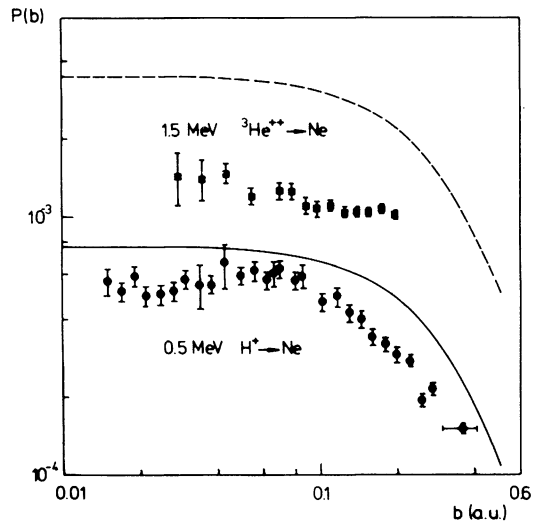

Fig.5.
Impact-parameter distribution of the cusp electrons within $\vartheta_f \leq 3°$ in 0.5 MeV/N H^+ + Ne and $^3He^{2+}$ + Ne collisions. The experimental data[14] are obtained by integrating the electron spectrum over the peak region. The calculations are performed with the fully peaked prior IA (integrated over the region $k_f = v \pm 0.1v$) and scaled down by a factor of 0.4 (solid line) and 0.23 (dashed line), respectively (see text)

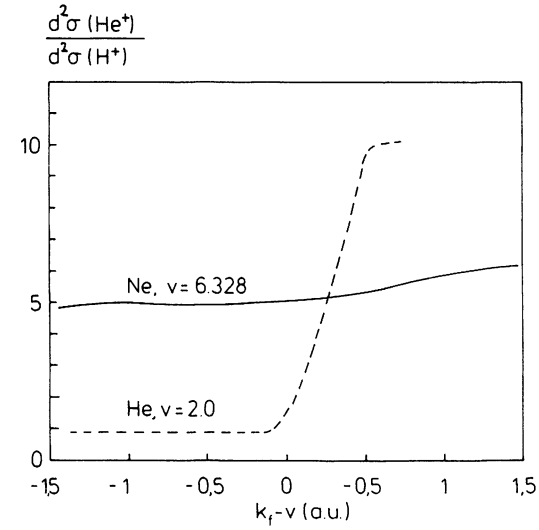

Fig.6.
Ratio of the doubly differential cross section for 100 keV/N He^+ + He to H^+ + He at $\vartheta_f = 5°$ within the Monte Carlo method[10] (dashed line) and for 1 MeV/N He^+ + Ne to H^+ + Ne for $\Theta_o = 1°$ within the fully peaked prior IA (solid line) as a function of electron momentum relative to v

target L-shell which yields the dominant contribution.

4. CTC by partly stripped projectiles

To simplify the theoretical description of the cusp electrons when the projectile carries electrons it is often assumed that the projectile acts like a pointlike particle of ionic charge. From the general theory (e.g. eq. (2.6)) it follows that the projectile field enters twofold, first directly as a transition operator in the matrix element, and second, implicitly in the final-state electronic wavefunction $\tilde{\varphi}^P_{fi}$. In Fig.6 is shown the doubly differential cross section ratio for He^+ + He relative to the H^+ + He collision system at an intermediate collision velocity of 2 au from a CTMC calculation when a static screened projectile field is used[10]. For small electron momenta, $k_f < v$, the ratio is approximately one which is conform with the picture of an ionic point charge. For $k_f > v$, however, He^+ is much more efficient in producing CTC cusp electrons than H^+. This is related to the fact that fast electrons require a large momentum transfer q, which is easier provided by the static screened He^+ potential which in the limit of $q \to \infty$ coincides with the He^{2+} field. Also shown in Fig.6 is the ratio for He^+ + Ne relative to H^+ + Ne in a fast collision (v = 6.328 au) from the (prior) peaked impulse approximation. A ratio of 4 is expected since the projectile field in the ionisation matrix element in (2.6) acts very much like a He^{2+} field for the large momenta required. The deviation of the ratio from 4 results from the consideration of the ionic field (including polarisation and exchange) in the calculation of the final-state electronic wavefunction.

5. CTC by neutral projectiles

For a short-range potential no cusp behaviour for the CTC electrons is expected as long as the projectile remains in its ground state. If the final-state electronic wavefunction is taken as a scattering eigenstate of the projectile (calcu-

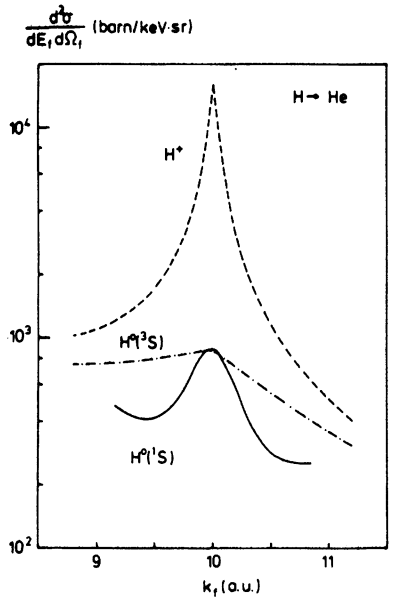

Fig.7.
Forward electron spectrum in 2.5 MeV H + He collisions for $\theta_0 = 0.5°$ within the fully peaked prior IA for different charge states of the projectile. - - - - , H^+, -·-·-·- , $H^0(^3S)$, ———, $H^0(^1S)$

lated from a Schrödinger-type equation including polarisation and exchange[16]) a forward peak is indeed obtained, although with a much larger width than in case of an ionic potential. Fig.7 displays the forward peak for neutral hydrogen projectiles in the spin singlet and spin triplet state in comparison with H^+ on a He target. The calculations are performed within the (prior) peaked impulse approximation where from the final-state wavefunction, only the l = 0 partial wave normalisation constant is required[17]. The existence of a peak for $\varkappa_f \longrightarrow 0$ results from the attractive polarisation potential, and the enhancement of the peak for the singlet state is due to the exchange interaction.

Experiments, where the projectile charge state is measured in coincidence with the electrons in order to isolate the CTC contribution show, however, a cusp-like structure even for neutral projectiles.[2] Fig.8 displays the forward peak in 75 keV/N H^0 + Ar and He^0 + Ar collisions separa-

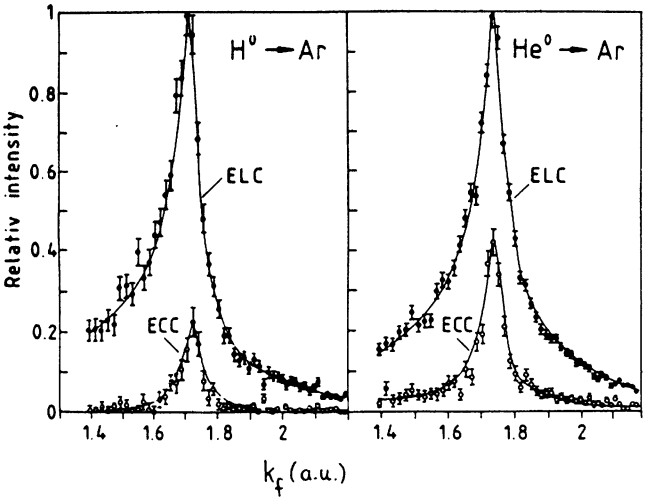

Fig.8.
Forward electron spectrum in 75 keV/N H^0 + Ar (left) and He^0 + Ar (right) collisions. Shown are the relative intensities for the electron loss contribution (ELC) and capture to continuum contribution (ECC) for $\theta_0 = 3.5°$. The solid lines are eye-guides to the data (taken from Ref.18)

ted into electron loss and electron capture contributions[18]. The fact that for the He^0 projectile, the cusp is even narrower than for a He^+ projectile has been tentatively explained in terms of a low-lying shape resonance[19]. In order to observe such a resonance which introduces a singularity into the final-state electronic wavefunction it is, however, necessary that the projectile is excited to a specific state prior to the CTC process. For He^0, the metastable 2^1S state (which may be present in the beam) can account for the occurrence of a resonance[20]. For neutral hydrogen on the other hand, it is difficult to imagine in which way a specific excited resonance-supporting projectile state can be sufficiently strong populated: From Fig.8 it follows that the peak intensity for CTC is about 20% of that for ELC. Assuming (optimistically) an equal transition probability for electron loss and electron capture by a projectile with fixed electronic configuration, the excitation probability of the projectile has to be as large as 0.2 !

In conclusion, it has been shown that the impulse approximation as well as the second Born theory are able to reproduce the features of the forward peak for energetic collisions with charged projectiles, such as the peak asymmetry and its dependence on velocity, projectile charge and angular acceptance. For neutral projectiles, the question of existence and interpretation of a cusp-like peak calls for further investigations.

Acknowledgments

The collaboration with W.Oswald (who provided the second Born results) and with the other members of the experimental group, H.-D.Betz and R.Schramm, is greatly acknowledged. I would also like to thank R.Koch and H.Schmidt-Böcking for providing the data on the b-distribution, and C.O.Reinhold for communicating the CTMC results prior to publication. Especially I would like to thank D.Berényi and his group for discussions and for their great hospitality during my visit in Debrecen.

References

1. Forward Electron Ejection in Ion-Atom Collisions, Lecture Notes in Physics, Vol. 213, eds. K.-O.Groeneveld, W.Meckbach and I.A. Sellin (Springer, Berlin 1984)
2. L.Sarkadi, J.Pálinkás, A.Kövér, D.Berényi and T.Vajnai, Phys.Rev.Lett. 62, 527 (1989)
3. H.Atan, W.Steckelmacher and M.W.Lucas, preprint (1989)
4. C.O.Reinhold and R.E.Olson, Phys.Rev. A39, 3861 (1989)
5. D.H.Jakubaßa-Amundsen, Int.J.Mod.Phys. A4, 769 (1989)
6. D.H.Jakubaßa-Amundsen, Phys.Rev. A38, 70 (1988)
7. W.Oswald, R.Schramm and H.-D.Betz, Phys.Rev. Lett. 62, 1114 (1989)
8. W.Meckbach, I.B.Nemirovsky and C.R.Garibotti, Phys.Rev. A24, 1793 (1981)
9. R.Shakeshaft and L.Spruch, Phys.Rev.Lett. 41, 1037 (1978)
10. C.O.Reinhold and D.R.Schultz, preprint (1989)
11. D.H.Jakubaßa-Amundsen, J.Phys. B16, 1761 (1983)
12. P.Dahl, J.Phys. B18, 1181 (1985)
13. D.K.Gibson and I.D.Reid, J.Phys. B19, 3265 (1986)
14. O.Jagutzki, R.Koch, A.Skutlartz and H.Schmidt-Böcking, Contributed Paper to the 3rd ECAMP, Bordeaux, Book of Abstracts p.654 (1989)
15. J.S.Briggs, J.Phys. B10, 3075 (1977)
16. H.Nakanishi and D.M.Schrader, Phys.Rev. A34, 1810 (1986)
17. D.H.Jakubaßa-Amundsen, J.Phys. B (in print)
18. A.Kövér, L.Sarkadi, J.Pálinkás, L.Gulyás, Gy.Szabó, T.Vajnai, D.Berényi, O.Heil, K.-O. Groeneveld, J.Gibbons and I.A.Sellin, preprint (1989)
19. C.R.Garibotti and R.O.Barrachina, Phys.Rev. A28, 2792 (1983)
20. R.O.Barrachina, preprint (1989)